The Astrophysical Journal, 835:237 (8pp), 2017 February 1 doi:10.3847/1538-4357/835/2/237

EBL Inhomogeneity and Hard-Spectrum Gamma-Ray Sources

Hassan Abdalla[1,2] and Markus Böttcher[1]
[1] Centre for Space Research, North-West University, Potchefstroom 2520, South Africa
[2] Department of Astronomy and Meteorology, Omdurman Islamic University, Omdurman 382, Sudan
Received 2016 August 5; revised 2016 November 30; accepted 2016 December 10; published 2017 January 31

Abstract

The unexpectedly hard very-high-energy (VHE; $E > 100$ GeV) γ-ray spectra of a few distant blazars have been interpreted as evidence of a reduction of the $\gamma\gamma$ opacity of the universe due to the interaction of VHE γ-rays with the extragalactic background light (EBL) compared to the expectation from current knowledge of the density and cosmological evolution of the EBL. One of the suggested solutions to this problem involves the inhomogeneity of the EBL. In this paper, we study the effects of such inhomogeneity on the energy density of the EBL (which then also becomes anisotropic) and the resulting $\gamma\gamma$ opacity. Specifically, we investigate the effects of cosmic voids along the line of sight to a distant blazar. We find that the effect of such voids on the $\gamma\gamma$ opacity, for any realistic void size, is only of the order of $\lesssim$1% and much smaller than expected from a simple linear scaling of the $\gamma\gamma$ opacity with the line-of-sight galaxy underdensity due to a cosmic void.

Key words: cosmology: miscellaneous – galaxies: active – galaxies: jets – radiation mechanisms: non-thermal

1. Introduction

Gamma rays from astronomical objects at cosmological distances with energies greater than the threshold energy for electron–positron pair production can be annihilated due to $\gamma\gamma$ absorption by low-energy extragalactic photons. The importance of this process for high-energy astrophysics was first pointed out by Nikishov (1962). In particular, very-high-energy (VHE; $E > 100$ GeV) γ-ray emission from blazars is subject to $\gamma\gamma$ absorption by the extragalactic background light (EBL), resulting in a high-energy cutoff in the γ-ray spectra of blazars (e.g., Stecker et al. 1992). The probability of absorption depends on the photon energy and the distance (redshift) of the source. Studies of intergalactic $\gamma\gamma$ absorption signatures have attracted further interest in astrophysics and cosmology, due to their potential use in probing the cluster environments of blazars (Sushch & Böttcher 2015) and in estimating cosmological parameters (Biteau & Williams 2015). However, bright foreground emissions prevent the accurate direct measurement of the EBL (Hauser & Dwek 2001). Studies of the EBL therefore focus on the predicted $\gamma\gamma$ absorption imprints and employ a variety of theoretical and empirical methods (e.g., Stecker 1969; Stecker et al. 1992; Aharonian et al. 2006; Franceschini et al. 2008; Razzaque et al. 2009; Finke et al. 2010; Dominguez et al. 2011a; Gilmore et al. 2012). All these cited works agree that the universe should be opaque (i.e., $\tau_{\gamma\gamma} \gtrsim 1$) to VHE γ-rays from extragalactic sources at high redshift ($z \gtrsim 1$).

Observations of distant ($z \gtrsim 0.5$) γ-ray blazars have been interpreted by some authors (e.g., MAGIC Collaboration et al. 2008; Archambault et al. 2014) as evidence that the universe may be more transparent to VHE γ-rays than expected based on all existing EBL models. Furthermore, several studies have found that, after correction for EBL absorption, the VHE γ-ray spectra of several blazars appear to be unexpectedly hard (photon indices $\Gamma_{\rm ph} \lesssim 1.5$) and/or exhibit marginal hints of spectral upturns toward the highest energies (e.g., Finke et al. 2010; Furniss et al. 2013). These unexpected VHE signatures in the spectra of distant blazars—although present only at marginal significance—are currently the subject of intensive research. Possible solutions include the hypothesis that the EBL density is generally lower than expected from current models (Furniss et al. 2013); the existence of exotic axionlike particles (ALPs) into which VHE γ-rays can oscillate in the presence of a magnetic field, thus enabling VHE photons to avoid $\gamma\gamma$ absorption (Dominguez et al. 2011b); an additional VHE γ-ray emission component due to interactions along the line of sight of extragalactic ultrahigh-energy cosmic rays originating from the blazar (e.g., Essey & Kusenko 2010); and EBL inhomogeneities. The idea of EBL inhomogeneities was considered by Furniss et al. (2015), who found tentative hints of correlations between hard VHE γ-ray sources and underdense regions along the line of sight. They suggested a direct, linear scaling of the EBL $\gamma\gamma$ opacity with the line-of-sight galaxy number density. The effect of EBL inhomogeneities on the $\gamma\gamma$ opacity was also investigated by Kudoda & Faltenbacher (2016). However, in that work, EBL inhomogeneities were considered only as a modulation of the redshift dependence of the cosmic star formation rate, without a detailed examination of the geometrical effects of large-scale structures of the universe. Both Furniss et al. (2015) and Kudoda & Faltenbacher (2016) concluded that the possible reduction of the EBL $\gamma\gamma$ opacity due to inhomogeneities is likely negligible.

In this paper, we investigate the effect of cosmological inhomogeneities on the energy density of the EBL and the resulting $\gamma\gamma$ opacity with a detailed calculation of the inhomogeneous and anisotropic EBL in a realistic geometrical model setup. Specifically, we consider the effect of cosmic voids along the line of sight to a distant blazar and investigate the resulting inhomogeneous and anisotropic EBL radiation field. In Section 2, we describe the model setup and the method used to evaluate the EBL characteristics and the resulting $\gamma\gamma$ opacity. The results are presented in Section 3, where we also compare them to the results of a simple linear scaling of the EBL $\gamma\gamma$ opacity with the line-of-sight galaxy count density for the specific example of PKS 1424 +240. We summarize and discuss our results in Section 4.

2. Extragalactic Background Light (EBL) in the Presence of a Cosmic Void

Our calculations of the inhomogeneous EBL are based on a modified version of the formalism presented in Razzaque et al.

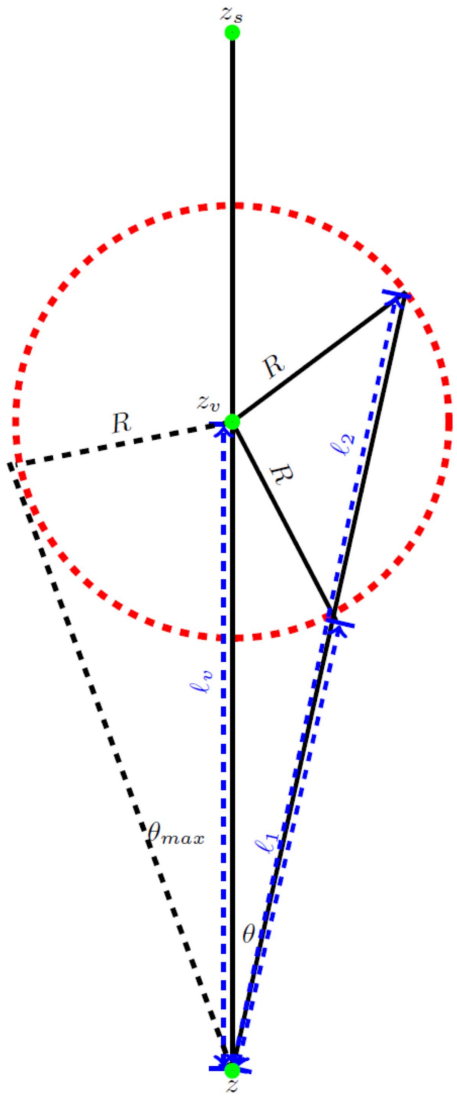

Figure 1. Illustration of an underdense region between the observer at redshift z and the source at redshift z_s. We assume that the underdense region has a radius R and the redshift at the center of the underdense region is z_v.

(2009), considering only the direct starlight. The effect of the reprocessing of starlight by dust has been included in Finke et al. (2010) and leads to an additional EBL component in the mid- to far-infrared, which is neglected here. Since dust reprocessing is a local effect, it is affected by cosmic inhomogeneities in the same way as the direct starlight contribution considered here.

For the purpose of a generic study of the effects of cosmic voids along the line of sight to a blazar, we start out by considering a single spherical cosmic void located, with its center at redshift z_v and with radius R, between the observer and a γ-ray source at redshift z_s. The geometry is illustrated in Figure 1. We calculate the angle-dependent and photon-energy-dependent EBL energy density at each point between the observer and the source by using comoving coordinates, converting redshifts z to distances $l(z)$. The cosmic void is represented by setting the star formation rate to 0 within the volume of the void.

For the evaluation of the differential EBL photon number density spectrum at a given redshift z, we modify the expression from Razzaque et al. (2009), based on the direct contribution from stars throughout cosmic history:

$$\frac{dN(\epsilon, z)}{d\Omega d\epsilon dV} = \int_{\tilde{z}=z}^{\infty} d\tilde{z} \left| \frac{dt}{d\tilde{z}} \right| \Psi(\tilde{z}) f_{\rm void}(\Omega, \tilde{z}) \times \int_{M_{\rm min}}^{M_{\rm max}} dM \left(\frac{dN}{dM} \right) \times \int_{\max\{0, z_d(M,z')\}}^{\tilde{z}} dz' \left| \frac{dt}{dz'} \right| f_{\rm esc}(\epsilon') \times \frac{dN(\epsilon', M)}{d\epsilon' dt}(1+z'), \quad (1)$$

where Ω represents the solid angle with respect to the photon propagation direction and $f_{\rm void}(\Omega, \tilde{z})$ is the step function set to zero within the void, as specified below. $\Psi(\tilde{z})$ is the cosmic star formation rate, dN/dM is the stellar mass function, $dN(\epsilon', M)/(d\epsilon'\, dt)$ is the stellar emissivity function, and $f_{\rm esc}(\epsilon')$ is the photon escape probability, for which we use the parameterizations of Razzaque et al. (2009). $dt/d\tilde{z}$ is evaluated using a concordance cosmology with $\Omega_m = 0.3$, $\Omega_\Lambda = 0.7$, and $h = 0.7$, and we define $\tilde{\ell}$ as the coordinate distance between z and $\tilde{z}$.

From Figure 1 we can find the distances l_1 and l_2, where the gamma-ray propagation direction Ω crosses the boundaries of the void:

$$\ell_{1,2} = \ell_v \mu \mp \sqrt{R^2 - \ell_v^2 \sin^2\theta}. \quad (2)$$

Here $\mu = \cos\theta$ is the cosine of the angle between the line of sight and the gamma-ray propagation direction, $\Omega = (\theta, \phi)$. The maximum angle $\theta_{\rm max}$ at which the gamma-ray travel direction still crosses the boundary at one point is given by

$$\sin\theta_{\rm max} = \frac{R}{\ell_v}. \quad (3)$$

The corresponding distance to the tangential point, $\ell_{\rm max}$, is given by

$$\ell_{\rm max} = \ell_v \cos\theta_{\rm max}. \quad (4)$$

The void condition can now be written as

$$f_{\rm void}^{\rm outside} = \begin{cases} 0 & \text{if } \ell_1 < \tilde{\ell} < \ell_2 \\ 1 & \text{else} \end{cases}$$

for points z along the line of sight that are located outside the void and

$$f_{\rm void}^{\rm inside} = \begin{cases} 0 & \text{if } \tilde{\ell} < \ell_2 \\ 1 & \text{else} \end{cases}$$

for points z along the line of sight located inside the void. Note that although the star formation rate has been set to zero inside the void, the EBL is not zero there because of the contribution from the rest of the universe outside the void.

To calculate the EBL density in comoving coordinates, the photon energy and volume can be transformed as $\epsilon_1 = \epsilon(1+z_1)$ and $V_1 = V/(1+z_1)^3$, respectively. Based on Equation (1), the EBL energy density can then be written as

(Razzaque et al. 2009)

$$\epsilon_1 \mu_{\epsilon_1}(\epsilon_1, z_1, \Omega) = (1 + z_1)^4 \, \epsilon^2 \, \frac{dN(\epsilon, z = z_1)}{d\Omega \, d\epsilon \, dV}. \quad (5)$$

With this expression for the EBL energy density, we can calculate the optical depth due to $\gamma\gamma$ absorption for a γ-ray photon from a source at redshift z_s with observed energy E as (Gould & Schréder 1967)

$$\tau_{\gamma\gamma}(E, z_s) = c \int_0^{z_s} dz_1 \left| \frac{dt}{dz_1} \right| \oint d\Omega \int_0^{\infty} d\epsilon_1 \times \frac{\mu_{\epsilon_1}(\epsilon_1, z_1, \Omega)}{\epsilon_1} (1 - \mu) \sigma_{\gamma\gamma}(s). \quad (6)$$

The $\gamma\gamma$ pair production cross-section $\sigma_{\gamma\gamma}(s)$ can be written as

$$\sigma_{\gamma\gamma}(s) = \frac{1}{2} \pi r_e^2 (1 - \beta_{\rm cm}^2) \Bigg[(3 - \beta_{\rm cm}^4) \ln \left(\frac{1 + \beta_{\rm cm}}{1 - \beta_{\rm cm}} \right) - 2\beta_{\rm cm}(2 - \beta_{\rm cm}^2) \Bigg] H\left(\frac{(1 + z_1) E \epsilon_1 (1 - \mu)}{2(m_e c^2)^2} - 1 \right), \quad (7)$$

where r_e is the classical electron radius, $\beta_{\rm cm} = \left(1 - \frac{1}{s}\right)^{1/2}$ is the electron–positron velocity in the center-of-momentum (c.m.) frame of the $\gamma\gamma$ interaction, $s = \frac{s_0}{2}(1 - \cos\theta)$ is the c.m. frame electron/positron energy squared, $s_0 = \frac{\epsilon E}{m_e^2 c^4}$, and H is the Heaviside function. $H(x) = 1$ if $x \geqslant 0$, and $H(x) = 0$ otherwise, representing the threshold condition that pair production can only occur if $\frac{(1 + z_1) E \epsilon_1 (1 - \mu)}{2(m_e c^2)^2} > 1$.

In the case of a homogeneous and isotropic EBL (with which we will compare our results for the inhomogeneous EBL case), Equation (6) can be simplified using the dimensionless function $\bar{\varphi}$ defined by Gould & Schréder (1967):

$$\bar{\varphi}[s_0(\epsilon)] = \int_1^{s_0(\epsilon)} s \bar{\sigma}(s) ds,$$

where $\bar{\sigma}(s) = \frac{2\sigma(s)}{\pi r_e^2}$ and $s_0(\epsilon) = E(1 + z)\epsilon / m_e^2 c^4$, so that Equation (6) reduces to Equation (17) in Razzaque et al. (2009):

$$\tau_{\gamma\gamma}^{\rm hom}(E, z) = c \, \pi r_e^2 \left(\frac{m_e^2 c^4}{E} \right)^2 \int_0^{z_s} \frac{dz_1}{(1 + z_1)^2} \left| \frac{dt}{dz_1} \right| \times \int_{\frac{m_e^2 c^4}{E(1+z1)}}^{\infty} d\epsilon_1 \frac{\mu_{\epsilon_1}}{\epsilon_1^3} \bar{\varphi}[s_0(\epsilon)]. \quad (8)$$

Knowing the optical depth $\tau_{\gamma\gamma}$, we can calculate the attenuation of the intrinsic photon flux $F_\nu^{\rm int}$ as

$$F_\nu^{\rm obs} = F_\nu^{\rm int} e^{-\tau_{\gamma\gamma}(E,z)}, \quad (9)$$

where $F_\nu^{\rm obs}$ is the observed spectrum.

3. Results

3.1. General Parameter Study: Single Void

We first investigate the effect of a single cosmic void along the line of sight to a distant γ-ray source on the resulting angle-averaged EBL energy density. Figure 2 (top panels) compares the EBL energy density spectrum (note that only the direct starlight contribution is accounted for) in the case of a void (dashed lines) to that in a homogeneous case (solid lines) for a spherical void of radius $R = 50\,h^{-1}$ Mpc (left panels) and $R = 100\,h^{-1}$ Mpc (right panels) at different points (redshifts, as indicated by the labels) along the line of sight. The center of the void is assumed to be located at a redshift of $z_v = 0.5$, considering a source located at redshift $z_s \geqslant 0.6$. The bottom panels of Figure 2 show the fractional difference between the homogeneous and inhomogeneous cases as a function of photon energy for various redshifts along the line of sight for the same two cases. As expected, the effect of the void is strongest right in the center of the void, but even there, it does not exceed a few percent (maximum fractional deficit ~7% in the $R = 100\,h^{-1}$ Mpc case). The effect generally increases with photon energy. The reason is that high-energy photons are produced primarily by high-mass stars and thus trace the most recent star formation history, which, for points within the void, is zero up to the time corresponding to the light travel time to the boundary of the void. As a function of position along the line of sight, the void-induced EBL deficit decreases approximately symmetrically for points in front of and behind the center of the void, with the slight asymmetry due to the $(1 + z_1)^4$ factor in Equation (5).

Figure 3 illustrates the effect of the void on the differential EBL energy density as a function of distance along the line of sight to the γ-ray source for two representative EBL photon energies, in the near IR ($\epsilon = 1$ eV) and near UV ($\epsilon = 8$ eV). The top panels show the absolute values of the energy densities, while the bottom panels show the fractional difference between the homogeneous and inhomogeneous cases. The figure illustrates that the maximum effect (at the center of the void) is approximately proportional to the size of the void but does not exceed ~7% in the case of the $R = 100\,h^{-1}$ Mpc void.

The relative EBL deficit as a function of distance is plotted for various different photon energies in the case of the $R = 50\,h^{-1}$ Mpc void on the left panel of Figure 4. The right panel of Figure 4 illustrates the angle dependence of the EBL in the presence of a void, compared to the homogeneous case. Right in the center of the void ($z_v = 0.5$ in the example studied here), the EBL is isotropic, due to the assumption of a spherical void, but is reduced compared to the homogeneous EBL case. For positions located outside the void, reduction is present only for EBL photon arrival directions intersecting the void, as expected.

Figure 5 illustrates the effect of a void on the $\gamma\gamma$ opacity for the same two example cases illustrated in Figure 2, for sources located at various redshifts in front of, within, and behind the void. As expected, the effect is negligible if the source is located in front of the void (as seen by an observer on Earth), and is at its maximum for source locations right behind the void. However, even in the case of the $R = 100\,h^{-1}$ Mpc void, the maximum effect on the $\gamma\gamma$ opacity is less than 1%. Note that the effect on the $\gamma\gamma$ opacity is much smaller than the maximum EBL energy density deficit in the center of the void, due to the integration over the entire line of sight.

3.2. Multiple Voids along the Line of Sight

After investigating the effect of a single cosmic void along the line of sight, we now investigate the more realistic case of several voids along (or near) the line of sight. From Figure 3, we notice that the relative EBL energy density deficit scales approximately proportionally to the size of the void. We therefore conclude that the effect of a number n of voids of

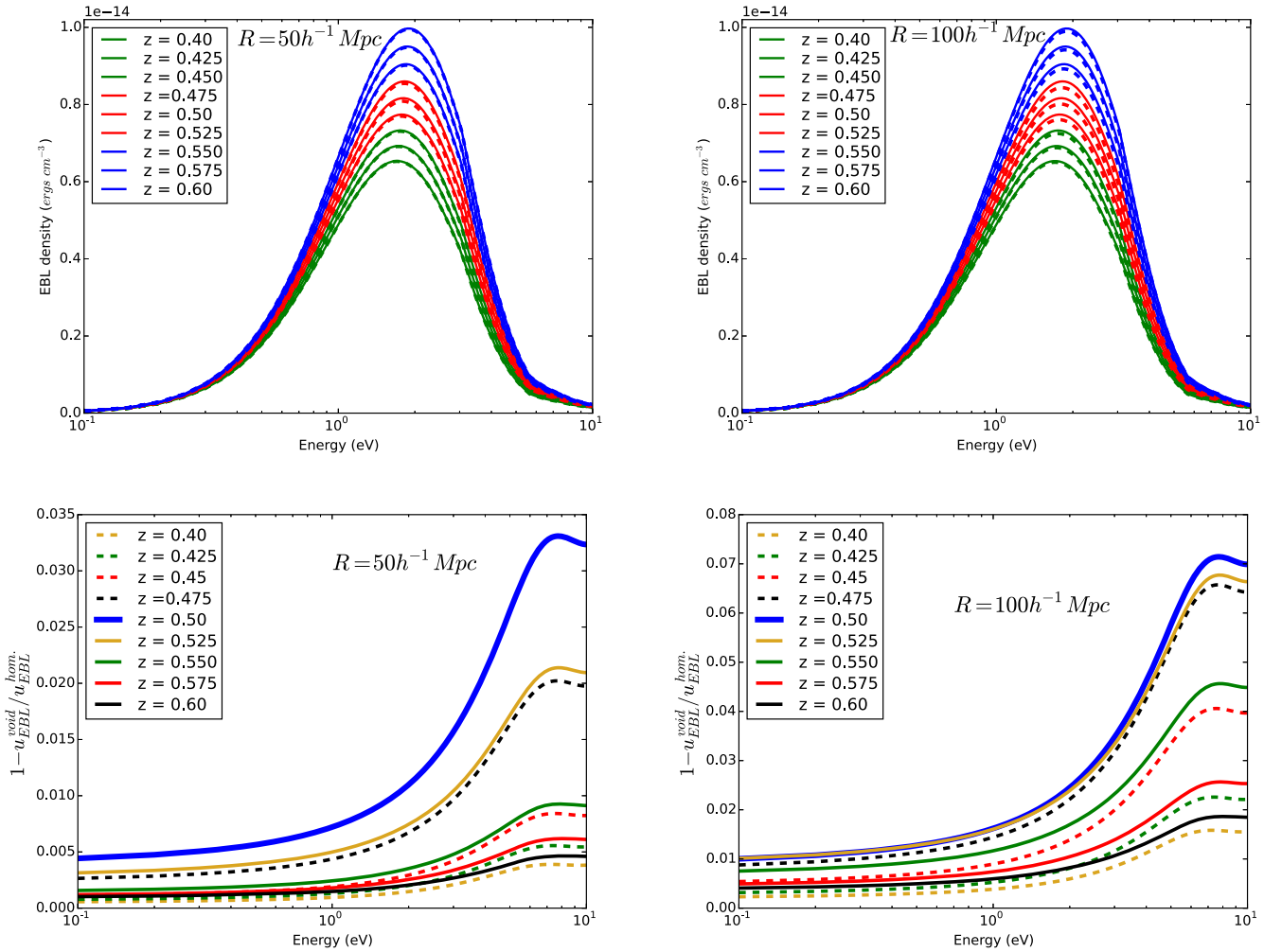

Figure 2. Top panels: angle-averaged EBL photon energy density spectra for a homogeneous EBL (solid lines) and in the presence of a spherical cosmic void (dashed lines) with its center at redshift $z_v = 0.5$ (comoving distance of 1.724 Gpc) and with radius $R = 50\,h^{-1}$ Mpc (left) and $R = 100\,h^{-1}$ (right). Green curves indicate locations in front of the void, red curves those within the void, and blue curves those behind the void. Bottom panels: relative deficit of the EBL energy density due to the void.

radius R_1 is approximately the same as the effect of a large void with radius $R_n = n\,R_1$. We therefore consider, as a test case, void sizes up to $R \lesssim 1\,h^{-1}$ Gpc, which approximate the effect of $\lesssim$10 voids with realistic void sizes $R \lesssim 100\,h^{-1}$ Mpc distributed along or very close to the line of sight. The center of the cumulative void is assumed to be located at a redshift of $z_v = 0.3$, given a source located at redshift $z_s \geqslant 0.6$.

Figure 6 (top left panel) compares the EBL energy density spectrum for such an accumulation of voids (dashed lines) to that of the homogeneous EBL case (solid lines). The top right panel of Figure 6 shows the fractional difference between the homogeneous and inhomogeneous cases as a function of photon energy for various redshifts along the line of sight. In the bottom left panel of Figure 6, we compare the resulting $\gamma\gamma$ opacities for the case of an ensemble of voids (dashed lines) and the homogeneous EBL case (solid lines), and the bottom right panel shows the $\gamma\gamma$ optical depth deficit due to the presence of voids for the same two cases on the left panel.

We note that for the extreme case of an accumulation of about 10 voids of typical sizes along the line of sight to a blazar, the EBL energy density even at the center of the cumulative void is reduced by around 35%, and the resulting maximum $\gamma\gamma$ opacity is reduced by around 15%. The reason is that even if the star formation rate is set to zero within the void, the EBL density within the void is still substantial due to the contributions from the rest of the universe outside the void.

3.3. Application to PKS 1424+240

Furniss et al. (2015) investigated the possibility that the unusually hard VHE γ-ray spectra observed in some distant ($z \gtrsim 0.5$) γ-ray blazars are due to a reduced EBL density caused by galaxy underdensities along the line of sight. Specifically, they investigated a possible correlation between galaxy count underdensities based on the Sloan Digital Sky Survey and the positions of hard-spectrum VHE blazars and found a tentative hint for such a correlation (although the small sample size prevented the authors from drawing firm conclusions). Based on this result, as a first estimate of the effect of such underdensities on the EBL, they suggested a linear scaling of the line-of-sight galaxy density with the EBL $\gamma\gamma$ opacity. For the specific case of the distant ($z \geqslant 0.6$; Furniss et al. 2013) VHE blazar PKS 1424+240, they found that the reduction of the EBL resulting from such a direct linear scaling is not sufficient to remove the apparent spectral hardening of the

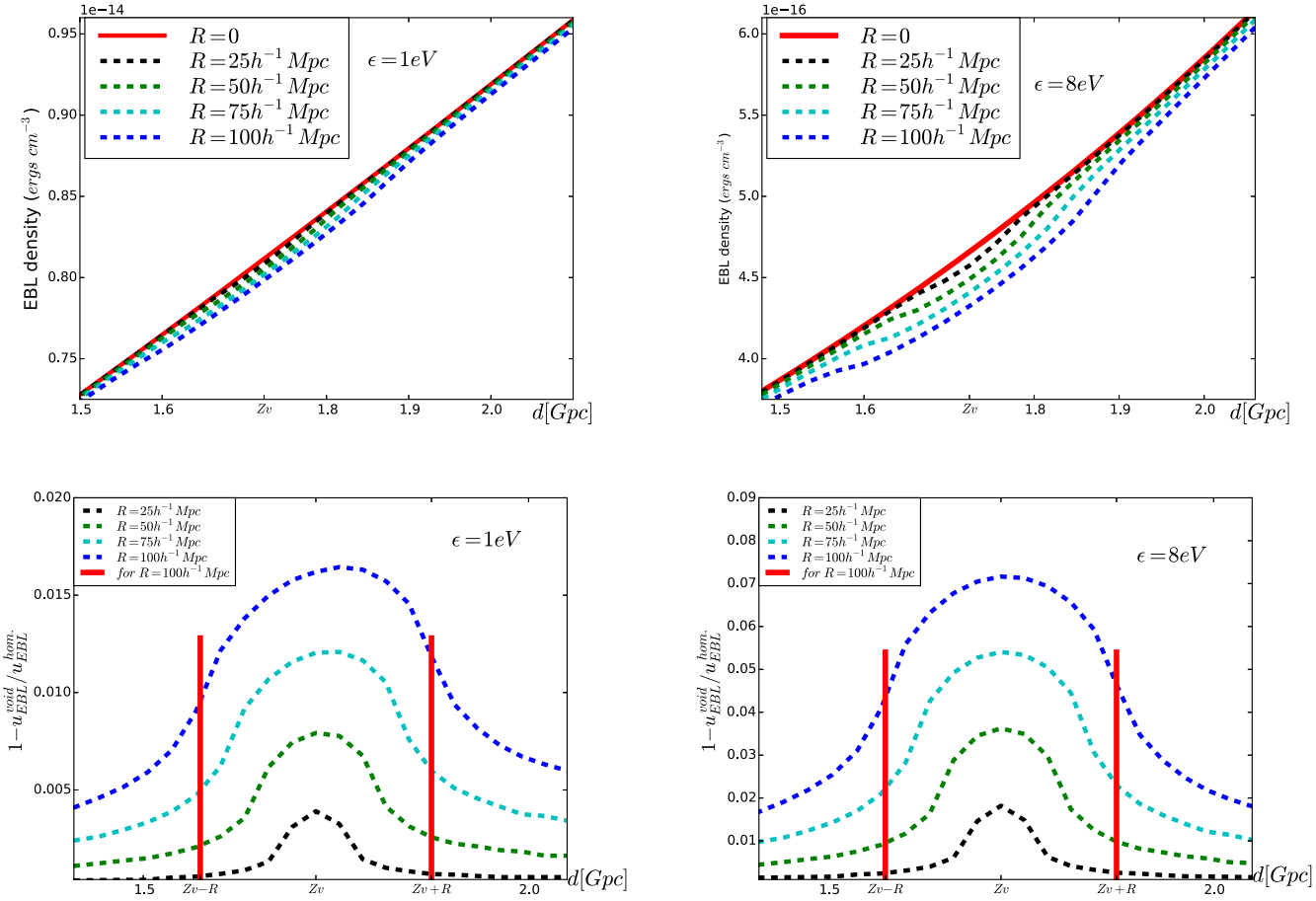

Figure 3. Top panels: differential EBL photon energy density as a function of distance along the line of sight for various sizes (as indicated by the labels) of a void located at $z_v = 0.5$ at two representative photon energies of $\epsilon = 1$ eV (left) and $\epsilon = 8$ eV (right). The red solid lines ($R = 0$) represent the homogeneous case. The general increase of the EBL energy density with redshift is due to the $(1 + z_1)^4$ factor in Equation (5) and the increase in star formation rate with redshift. Bottom panels: relative EBL energy density deficit due to the presence of a void for the same cases as in the top panels. The red vertical lines indicate the boundaries of the void for the $R = 100\,h^{-1}$ Mpc case.

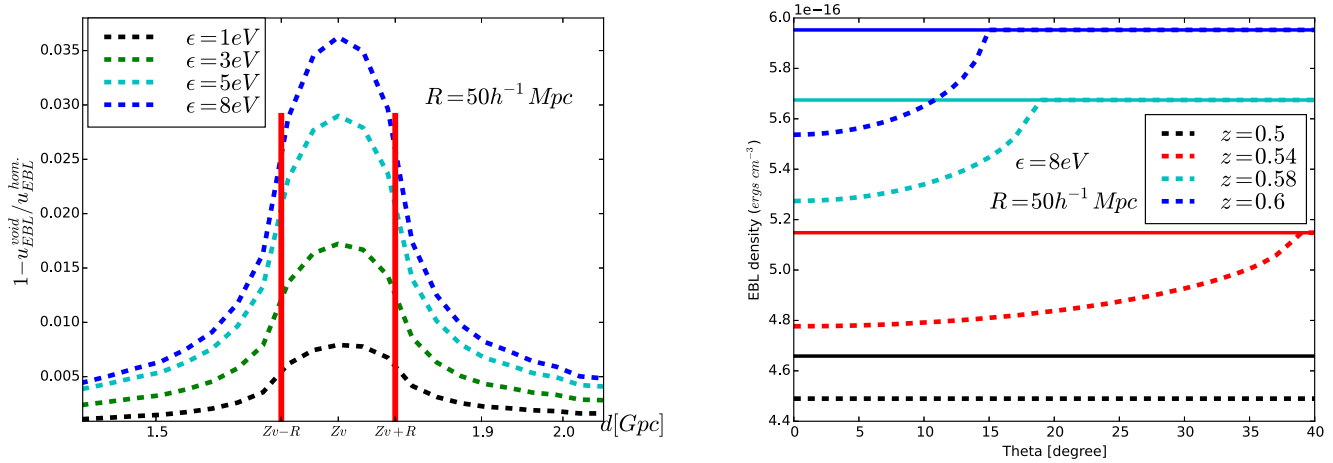

Figure 4. Left panel: relative differential EBL energy density deficit as a function of distance along the line of sight for various EBL photon energy densities in the case of an $R = 50\,h^{-1}$ Mpc void located at $z_v = 0.5$. The red vertical lines indicate the boundaries of the void. Right panel: angle dependence (θ is the angle with respect to the direct line of sight through the center of the void) of the EBL energy density in the presence of an $R = 50\,h^{-1}$ Mpc at the $z_v = 0.5$ void (dashed lines), compared to the homogeneous case (which does not have any angle dependence; solid lines), at a representative near-UV photon energy of $\epsilon = 8$ eV for three positions (redshifts) along the line of sight: at the center of the void (black, lower curves), within the void but behind its center (red curves), and behind the void (blue and cyan, upper curves).

VHE γ-ray spectrum observed by VERITAS when correcting for EBL absorption based on state-of-the-art (homogeneous) EBL models (Archambault et al. 2014).

For an assumed redshift of $z = 0.6$ for PKS 1424+240, our example case of $R = 50\,h^{-1}$ Mpc and $z_v = 0.5$ results in approximately the same galaxy count underdensity factor found

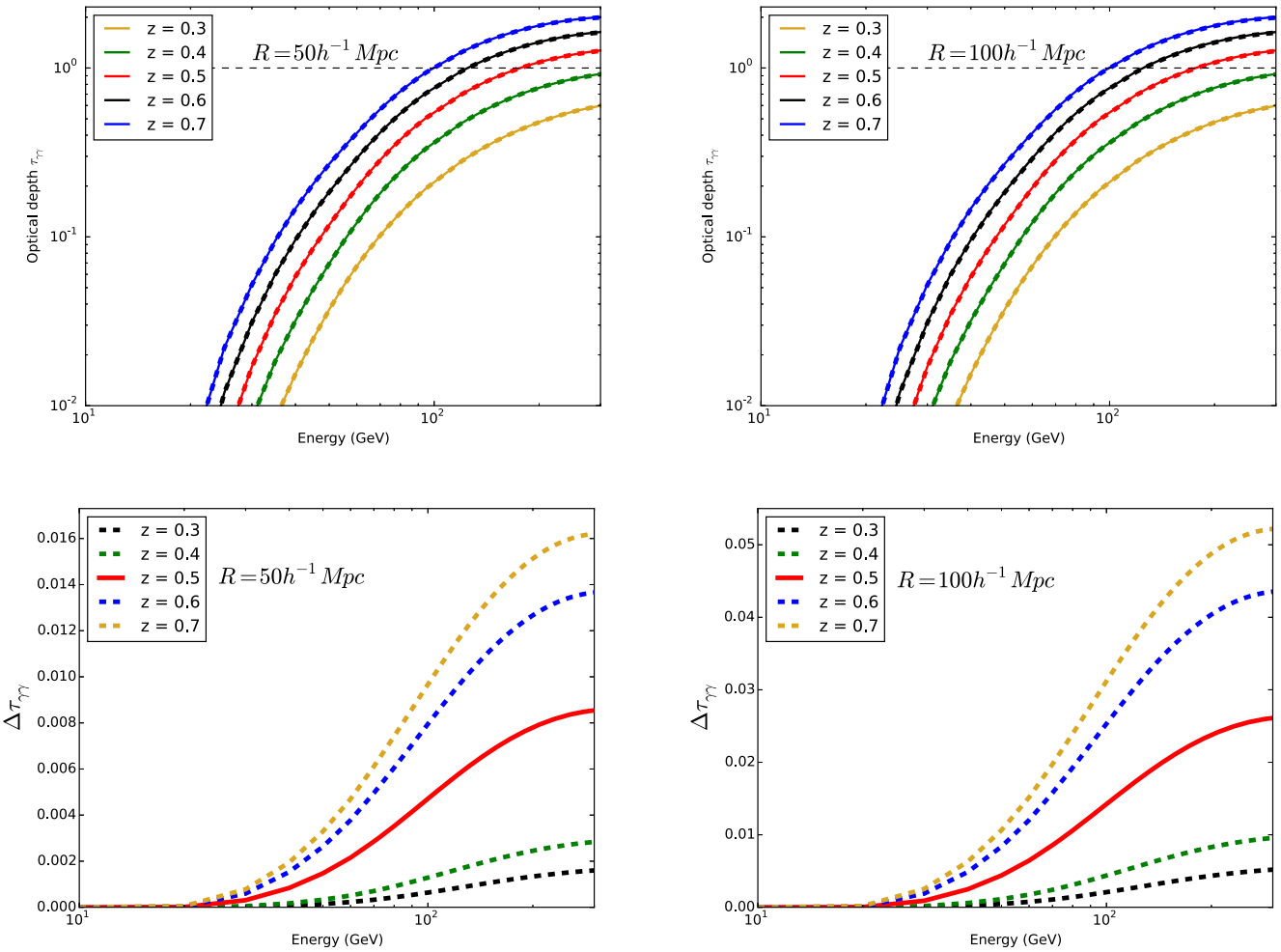

Figure 5. Top panels: EBL $\gamma\gamma$ optical depth as a function of γ-ray photon energy in the presence of a void (dashed), compared to the homogeneous case (solid), for the same example voids illustrated in Figure 2. Bottom panels: $\gamma\gamma$ optical depth deficit due to the presence of voids for the same two cases on the top panels.

by Furniss et al. (2015) along the line of sight to this source. Therefore, in Figure 7, we compare the EBL reduction effect based on direct linear scaling with galaxy underdensity, with our detailed EBL calculation assuming a void along the line of sight, for the two observing periods presented in Archambault et al. (2014). The left panel illustrates the effect on the actual νF_ν spectra, while the right panel shows the γ-ray spectra normalized to the flux points corrected by the homogeneous Gilmore et al. (2012) EBL absorption model. The figure illustrates that the EBL opacity reduction effect due to the void in our detailed calculations is slightly smaller than the effect from a direct linear scaling with galaxy underdensity. Thus, we conclude that the tentative spectral hardening of the VHE spectrum of PKS 1424+240 is likely not an artifact of an underestimate of the EBL opacity due to possible EBL inhomogeneities.

4. Summary and Conclusions

We have presented detailed calculations of the effect of cosmic inhomogeneities on the EBL and the resulting $\gamma\gamma$ opacity for VHE γ-ray photons from sources at cosmological distances. Specifically, we have considered the presence of a cosmic void, which, for simplicity, we have represented as a spherical region in which the local star formation rate is zero. We have shown that for realistic void sizes of $R \lesssim 100\,h^{-1}$ Mpc, the EBL energy density even at the center of the void is reduced by less than 10%. Even if the void is located right in front of the background γ-ray source, the $\gamma\gamma$ opacity is reduced by typically less than 1%. We find an approximately linear scaling of the EBL deficit effect with the size of the void. Even in the presence of a large number of voids adding up to a total line-of-sight distance through voids of $\sim 2\,h^{-1}$ Gpc ($=2\,R_n$), the EBL $\gamma\gamma$ opacity is only reduced by $\sim$15%.

This reduction is smaller than that obtained from a direct linear scaling of the $\gamma\gamma$ opacity with galaxy count underdensities along the line of sight to γ-ray sources. For the specific case of PKS 1424+240, we have illustrated that the inferred (marginal) spectral hardening of the VHE γ-ray spectrum, after correction for EBL absorption, is most likely not an artifact of an overestimation of the EBL opacity due to cosmic inhomogeneities—if confirmed by future, more sensitive VHE γ-ray observations.

Since we have shown that realistic EBL inhomogeneities do not lead to a significant reduction of the EBL $\gamma\gamma$ opacity, hints for the unexpected hardening of the VHE spectra of several blazars remain, for which other explanations would have to be invoked, if they can be confirmed by future observations (e.g., by the Cherenkov Telescope Array). One possibility is that this hardening is, in fact, a real, intrinsic feature of the γ-ray spectra of these blazars, possibly due to a pion-production-induced cascade component in a hadronic blazar model scenario (e.g.,

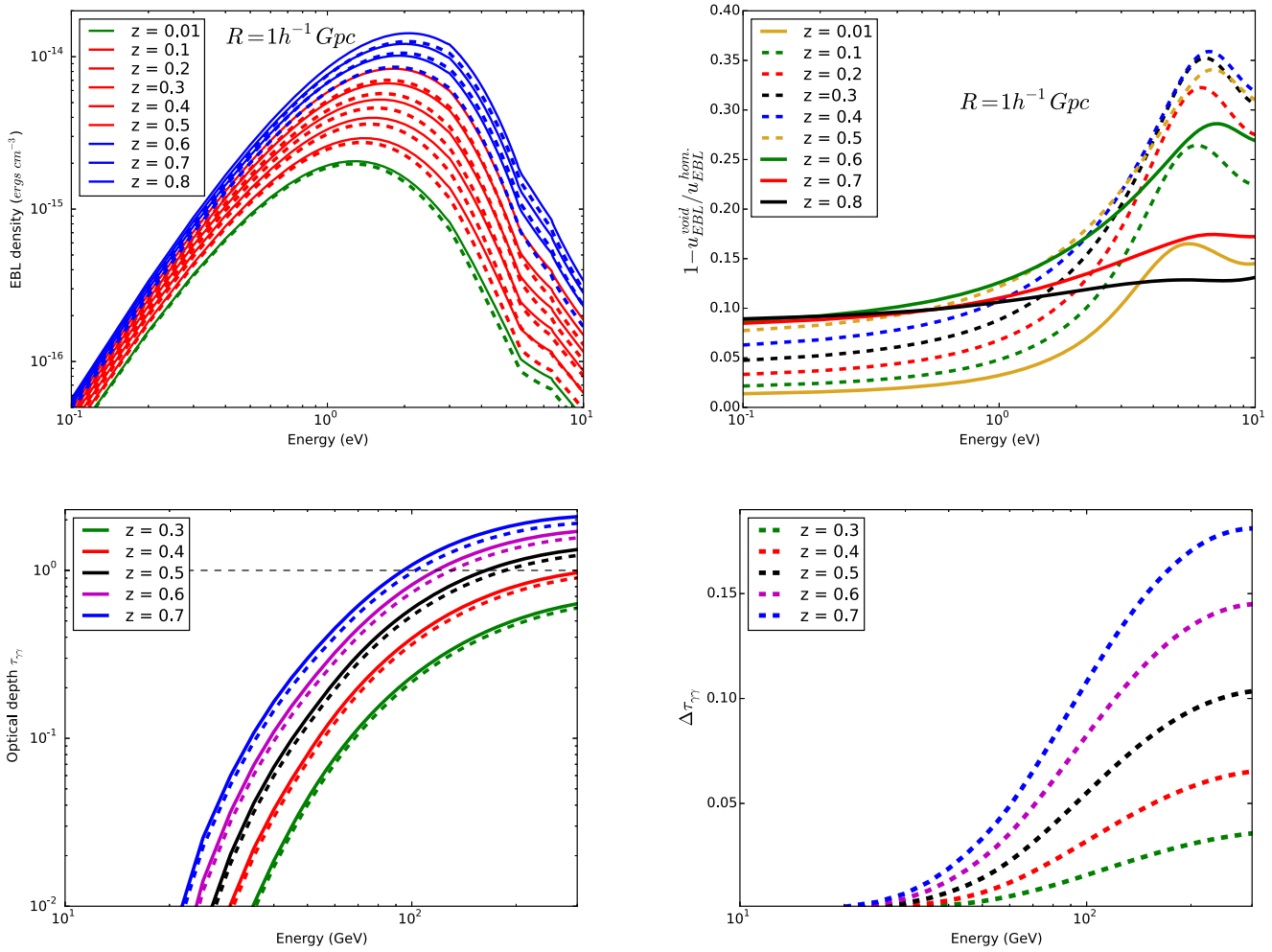

Figure 6. Top left panel: angle-averaged EBL photon energy density spectra for a homogeneous EBL (solid lines) and in the presence of an accumulation of 10 cosmic voids of radius $R = 100\ h^{-1}$ Mpc each (dashed lines), whose distribution along the line of sight is centered at redshift $z_v = 0.3$. Green curves indicate locations in front of the ensemble of voids, red curves locations within, and blue curves locations behind. Top right panel: relative deficit of the EBL energy density due to the voids; dashed lines and solid lines represent the effect of voids on the EBL energy density inside and outside the ensemble of voids, respectively. Bottom left panels: EBL $\gamma\gamma$ optical depth as a function of γ-ray photon energy in the presence of voids (dashed), compared to the homogeneous case (solid), for the same example voids illustrated in the top panels. Bottom right panels: $\gamma\gamma$ optical depth deficit due to the presence of voids for the same two cases on the left panel.

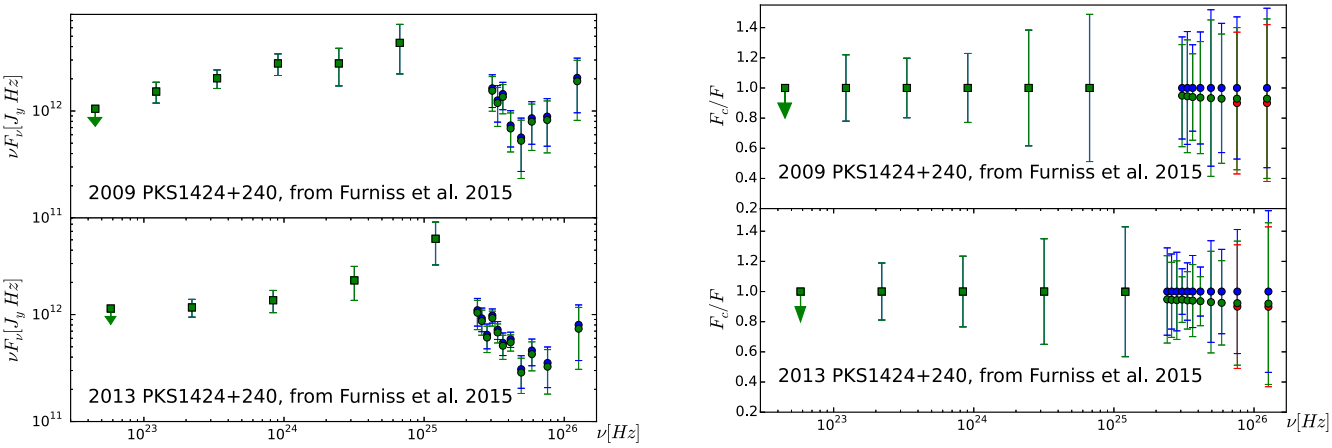

Figure 7. HE–VHE γ-ray spectra of PKS 1424+240 from Archambault et al. (2014). The blue points show the EBL-corrected spectrum using the Gilmore et al. (2012) EBL model. The red points represent the reduced EBL correction using the linear scaling of $\tau_{\gamma\gamma}$ with the line-of-sight galaxy density, as suggested by Furniss et al. (2015). The green points illustrate the reduced EBL correction resulting from our model calculation with a void of radius $R = 50\ h^{-1}$ Mpc centered at $z_v = 0.5$ (comoving distance of 1.724 Gpc), assuming a source redshift of $z_s = 0.6$ (comoving distance of 2.056 Gpc), which results in approximately the same perceived line-of-sight galaxy underdensity used by Furniss et al. (2015). The left panels show the actual νF_ν spectra, while the right panels show the spectra normalized to the EBL-corrected flux points from Archambault et al. (2014).

Böttcher et al. 2013; Cerruti et al. 2015). If such a spectral hardening is not intrinsic to the source, more exotic explanations, such as ALPs or a cosmic-ray induced secondary-radiation component, would need to be invoked.

We thank Amy Furniss for stimulating discussions and for sharing the PKS 1424+240 data with us. We also thank the anonymous referee for a careful reading of the manuscript and helpful suggestions, which have led to significant improvements of the manuscript. The work of M.B. is supported by the South African Research Chair Initiative of the National Research Foundation[3] and the Department of Science and Technology of South Africa, under SARChI Chair Grant No. 64789.

References

Aharonian, F., Akhperjanian, A. G., Bazer-Bachi, A. R., et al. 2006, Natur, 440, 1018
Archambault, S., Aune, T., Behera, B., et al. 2014, ApJL, 785, L16
Biteau, A., & Williams, D. A. 2015, ApJ, 812, 60
Böttcher, M., Reimer, A., Sweeney, K., & Prakash, A. 2013, ApJ, 768, 54
Cerruti, M., Zech, A., Boisson, C., & Inoue, S. 2015, MNRAS, 448, 910
Dominguez, A., Primack, J. R., Rosario, D. J., et al. 2011a, MNRAS, 410, 2556
Dominguez, A., Sánchez-Conde, M. A., & Prada, F. 2011b, JCAP, 11, 020
Essey, W., & Kusenko, A. 2010, APh, 33, 81
Finke, J. D., Razzaque, S., & Dermer, C. D. 2010, ApJ, 712, 238
Franceschini, A., Rodigheiro, G., & Vaccari, M. 2008, A&A, 487, 837
Furniss, A., Williams, D. A., Danforth, C., et al. 2013, ApJL, 768, L31
Furniss, A., Stutter, P. M., Primack, J. R., & Dominguez, A. 2015, MNRAS, 446, 2267
Gilmore, R. C., Sommerville, R. S., Primack, J. R., & Dominguez, A. 2012, MNRAS, 422, 3189
Gould, R. J., & Schréder, G. P. 1967, PhRv, 155, 1408
Hauser, M. G., & Dwek, E. 2001, ARA&A, 39, 249
Kudoda, A. M., & Faltenbacher, A. 2016, in 3rd Annual Conf. on High Energy Astrophysics in Southern Africa (HEASA2015), ed. S. Razzaque et al. (Trieste: Proceedings of Sciences), 20
MAGIC Collaboration, Albert, J., et al. 2008, Sci, 320, 1752
Nikishov, A. I. 1962, JETP, 14, 393
Razzaque, S., Demer, C. D., & Finke, J. D. 2009, ApJ, 697, 483
Stecker, F. W. 1969, ApJ, 157, 507
Stecker, F. W., de Jager, O. C., & Salamon, M. H. 1992, ApJL, 390, L49
Sushch, I., & Böttcher, M. 2015, A&A, 573, A47

[3] Any opinion, finding, or conclusion or recommendation expressed in this material is that of the authors, and the NRF does not accept any liability in this regard.